(1985) *Biochemistry 24*, 3012–3019.
Swallow, A. J. (1982) in *Function of Quinones in Energy Conserving Systems* (Trumpower, B. L., Ed.) pp 59–72, Academic Press, New York.
Takeuchi, H., & Harada, I. (1986) *Spectrochim. Acta 42A*, 1069–1078.
Ubbink, M., van Kleef, M. A. G., Kleinjan, D.-J., Hoitink, C. W. G., Huitema, F., Beintema, J. J., Duine, J. A., & Canters, G. W. (1991) *Eur. J. Biochem.* (in press).
van der Meer, R. A., Jongejan, J. A., & Duine, J. A. (1987) *FEBS Lett. 221*, 299–304.
van Wielink, J. E., Frank-Jzn, J., & Duine, J. A. (1990) *Methods Enzymol. 188*, 235–241.
Vellieux, F. M. D., Huitema, F., Groendijk, H., Kalk, K. H., Frank-Jzn, J., Jongejan, J. A., Duine, J. A., Petratos, K., Drenth, J., & Hol, W. G. J. (1989) *EMBO J. 8*, 2171–2178.

Iron Binding to Horse Spleen Apoferritin: A Vanadyl ENDOR Spin Probe Study†

Phillip M. Hanna,‡ N. Dennis Chasteen,*,‡ Gerald A. Rottman,§ and Philip Aisen*,§

Department of Chemistry, University of New Hampshire, Durham, New Hampshire 03824, and Department of Physiology and Biophysics, Albert Einstein College of Medicine, 1300 Morris Park Avenue, Bronx, New York 10461

Received May 24, 1991; Revised Manuscript Received July 8, 1991

ABSTRACT: The role of the protein shell in the formation of the hydrous ferric oxide core of ferritin is poorly understood. A VO^{2+} spin probe study was undertaken to characterize the initial complex of Fe^{2+} with horse spleen apoferritin (96% L-subunits). A competitive binding study of VO^{2+} and Fe^{2+} showed that the two metals compete 1:1 for binding at the same site or region of the protein. Curve fitting of the binding data showed that the affinity of VO^{2+} for the protein was 15 times that of Fe^{2+}. Electron nuclear double resonance (ENDOR) measurements on the VO^{2+}–apoferritin complex showed couplings from two nitrogen nuclei, tentatively ascribed to the N1 and N3 nitrogens of the imidazole ligand of histidine. The possibility that the observed nitrogen couplings are from two different ligands is not precluded by the data, however. A pair of exchangeable proton lines with a coupling of approximately 1 MHz is tentatively assigned to the NH proton of the coordinated nitrogen. A 30–40% reduction in the intensity of the ^1H matrix ENDOR line upon D_2O–H_2O exchange indicates that the metal-binding site is accessible to solvent and, therefore, to molecular oxygen as well. The ENDOR data provide the first evidence for a principle iron(II)-binding site with nitrogen coordination in an L-subunit ferritin. The site may be important in Fe^{2+} oxidation during the beginning stages of core formation.

From microorganisms to man, ferritin plays a central role in the biological management of iron (Ford et al., 1984; Clegg et al., 1980a; Crichton, 1973; Thiel, 1987, 1989). The protein consists of a hollow spherical protein shell of 24 nearly identical subunits encapsulating a hydrous ferric oxide mineral core (Ford et al., 1984). Ferritins consist of so called H (heavy) and L (light) subunits with similar molecular weights (ca. 20000) but slightly different mobilities on SDS–PAGE. There is 60–65% sequence homology between the two types of subunits (Theil, 1989). The horse spleen protein used in the present work consists of 96% L-subunits.

Eight hydrophilic and six hydrophobic channels penetrate the protein shell along 3-fold and 4-fold symmetry axes, respectively (Ford et al., 1984). The hydrophilic channels have been generally thought to be the ports through which iron enters and leaves the protein interior but recent work with recombinant H-chain ferritins has called this idea into question (Treffry et al., 1989). During deposition, iron enters the protein as Fe^{2+} and is subsequently oxidized to Fe^{3+}, becoming incorporated into the mineral core (Bryce & Crichton, 1973). In horse spleen apoferritin, Fe^{2+} binding and oxidation appear to be protein-assisted in the early stage of core development (Crichton & Roman, 1978; Paques et al., 1979). After sufficient core has developed, oxidation and deposition appears to occur directly on the growing mineral surface (Macara et al., 1972; Clegg et al., 1980a,b). An important "ferroxidase" site has recently been identified in human liver H-subunit apoferritin by using genetically engineered mutant proteins (Lawson et al., 1989, 1991; Levi et al., 1988, 1989). To date no such site has been identified on an L-subunit although L-subunit rich horse spleen ferritin is competent in oxidizing and storing iron.

The vanadyl ion is a useful paramagnetic probe of metal-binding sites in biological systems (Chasteen, 1981, 1983) and has been used in previous in vitro studies of apoferritin (Wardeska et al., 1986; Chasteen & Theil, 1982). Vanadyl complexes with ferritin are also of interest since they are known to occur in tissues of rats raised on a vanadium-supplemented diet (Chasteen et al., 1986a,b). In vitro room temperature EPR studies at pH 6.25 and 7.0 suggest that vanadyl binding in apoferritin occurs at or near sites that also bind Fe^{2+} and Fe^{3+} (Wardeska et al., 1986; Chasteen & Theil, 1982). Therefore, it appears that the vanadyl ion binds at one or more sites involved in iron accumulation in ferritin and may be used as a spectroscopic and mechanistic probe of these sites.

EPR spin Hamiltonian parameters suggest that the ligation about the bound VO^{2+} in apoferritin consists primarily of O-donor ligands (Chasteen, 1981; Chasteen & Theil, 1982). The vanadyl (d^1) unpaired electron occupies a nonbonding d_{xy} orbital in the ground state, resulting in ligand electron–nuclear hyperfine interactions that are generally too small to be observed in the EPR spectrum. These interactions may be measured, however, by electron–nuclear double resonance (ENDOR) spectroscopy.

† This work was supported by Grants 2 RO1 GM20194 (N.D.C.), 2 RO1 DK15056 (P.A.), and 1 K11 DK01841 (G.A.R.) from the National Institutes of Health.
* Authors to whom correspondence should be addressed.
‡ University of New Hampshire.
§ Albert Einstein College of Medicine.

0006-2960/91/0430-9210$02.50/0

In the present work, ENDOR spectroscopy provides the first evidence for a principle Fe^{2+}-binding site, which contains a nitrogen donor ligand(s), on an L-subunit ferritin. The ligand(s) is (are) tentatively ascribed to an imidazole group of histidine. Competitive binding experiments between Fe^{2+} and VO^{2+} carried out under more stringent oxygen-free conditions than those previously used (Chasteen & Theil, 1982) indicate 1:1 competition between the two metals. A mixture of oxygen and nitrogen donor ligands at the metal site makes it well suited for complexing both Fe^{2+} and Fe^{3+} and suggests that this site may play an important role in facilitating Fe^{2+} oxidation during the initial stages of iron deposition in apoferritin. The implications of these findings to the mechanism of iron incorporation are discussed, and a possible location for the site on the protein is suggested.

Materials and Methods

All chemicals were reagent grade or better and used without further purification unless otherwise indicated. Horse spleen ferritin (3× crystallized, cadmium free) and *Aspergillus niger* glucose oxidase (EC 1.1.3.4; grade 1) were purchased from Boehringer Mannheim Biochemicals. MES, MOPS, and HEPES[1] were purchased from Research Organics Inc.; cupric sulfate pentahydrate (99.0%) was from the Fisher Scientific Co.; disodium EDTA dihydrate and ferrous sulfate heptahydrate (99.8%) were from the J. T. Baker Chemical Co.; 95% thioglycolic acid, vanadyl sulfate trihydrate (99.99%), sodium chloride, and sodium dithionite were from the Aldrich Chemical Co.; and Chelex resin (dry mesh 50–100), bovine liver catalase (EC 1.11.1.6; 24.3 mg/mL), and β-D-(+)-glucose were from the Sigma Chemical Company.

Apoferritin was prepared by a previously published procedure using thioglycolic acid (Chasteen & Theil, 1982), modified according to the second variation described in Hanna et al. (1991). Chelex resin was used to demetalate buffer solutions, and all steps, except the ultrafiltration, were carried out at 4 °C. Apoferritin concentration was determined from its absorbance at 280 nm [ϵ = 19 500 M^{-1} cm^{-1} per subunit (Heusterspreute & Crichton, 1981)] and is reported here on a 24-mer basis. The apoprotein solution typically contained approximately 0.01 Fe/subunit as determined by atomic absorption analysis. The percentages of H and L subunits were determined by SDS–PAGE (Adelman et al., 1975). The Coomassie blue R250 stained gel was scanned with a Hoefer GS 300 scanning densitometer interfaced to a Digital Equipment Corp. MINC 11/23 computer.

Iron was added to apoferritin by using 0.1 or 0.02 M ferrous sulfate prepared in dilute H_2SO_4 (pH 1.5). The g' = 4.3 Fe^{3+}–apoferritin complex was completely formed within 10 min after aerobic addition of an appropriate amount of ferrous solution to apoferritin. Ferrous- and vanadyl–apoferritin EPR samples were prepared under anaerobic conditions with Ar (grade 4.8; WESCO, Billerica, MA) passed through two solutions of V^{2+} over zinc amalgam to remove trace O_2. Samples were purged for 1 h before any subsequent metal additions. After an appropriate incubation period (typically 10 min for each metal addition unless otherwise stated), the EPR samples were frozen in either liquid nitrogen or a dry-ice/acetone slush.

For stoichiometric binding studies involving titrations of the protein with metal ions, strict anaerobic conditions were necessary and were achieved by the addition of 0.72 mg/mL (57.5 units) glucose oxidase, 5 mM β-D-(+)-glucose, and 0.75 mg/mL (12 000 units) catalase 15 min prior to the addition of metal ions. In control experiments, no EPR signal with apoferritin was observed with the O_2-reducing glucose oxidase/glucose/catalase system nor was the VO^{2+}–apoferritin spectral line shape or binding stoichiometry affected by the presence of the system.

Apotransferrin was purchased from Calbiochem. The protein was dialyzed against 0.1 M $NaClO_4$ followed by 0.1 M HEPES, pH 7.4. The divanadyl protein complex was prepared by the addition of 0.05 M $VOSO_4$, pH 1.5, to the protein under a N_2 atmosphere as previously described (Cannon & Chasteen, 1975).

X-band (9.2–9.3 GHz) EPR spectra were recorded at liquid nitrogen temperatures on a Varian E-4 spectrometer interfaced to the MINC 11/23 computer for data acquisition and manipulation. Calibrated 3-mm i.d./4-mm o.d. quartz sample tubes were used for all EPR and ENDOR measurements. ENDOR spectra were recorded at 2.0–2.3 K with an IBM-Bruker ESR 200D-SRC spectrometer fitted with a Bruker EN810 ENDOR accessory and a 200 W ENI model 3200L rf amplifier. Temperature control was achieved with an Oxford ESR 10 cryostat mounted in the TM_{110} ENDOR cavity. Temperatures were measured before and after each run by using a Lake Shore Cryotronics thermometer with a glassy carbon probe.

Results

VO^{2+} and Fe^{2+} Competitive Binding Studies. Only mononuclear VO^{2+} bound to the protein exhibits an EPR signal at the pH values used in this work. [Uncomplexed vanadyl ions dimerize above pH 2 and oligomerize above pH 4.5 forming EPR-silent species (Chasteen, 1981).] The EPR spectra for apoferritin containing 8 VO^{2+} at pH 5.71 and 16 VO^{2+} at pH 7.36 are shown in the upper and lower panels of Figure 1, respectively. At any given pH, the EPR line shape remains independent of the amount of vanadyl ion added to the protein. The pH-related α and β forms of the VO^{2+}–apoferritin complex are evident for the sample at pH 7.36 (Figure 1, bottom), whereas the α form predominates at pH 5.71 (Figure 1, top) (Chasteen & Theil, 1982). The β form of the complex is thought to arise from the α form upon deprotonation of an aquo ligand (Chasteen & Theil, 1982; Gerfin et al., 1991).

A spectrometric titration curve for the competitive binding between VO^{2+} and Fe^{2+}, while monitoring the EPR amplitude of the VO^{2+}–protein complex, is shown in Figure 2. The attenuation of the VO^{2+} EPR signal with added Fe^{2+} indicates that VO^{2+} and Fe^{2+} compete for the same binding site or region on the protein. Similar results are obtained regardless of the order of addition of the metals (Figure 2, open and solid circles). The difference in the shape of the curve in Figure 2 from that reported previously (Chasteen & Theil, 1982), the lesser degree of VO^{2+} displacement by Fe^{2+}, and the independence of the binding isotherm on the order of addition of the two metals are probably the result of better maintenance of anaerobic conditions in the present work. The dependence of the previous data on the order of metal ion addition precluded analysis by an equilbrium binding model (Chasteen & Theil, 1982).

The improved binding data reported here were modeled by assuming a simple 1:1 competition between the two metals for a common binding site on the protein, P, namely

$$Fe^{2+} + VOP \overset{K}{\rightleftharpoons} FeP + VO^{2+} \quad (1)$$

[1] Abbreviations: ESEEM, electron spin echo envelope modulation; HEPES, *N*-(2-hydroxyethyl)piperazine-*N'*-(2-ethanesulfonic acid); MES, 2-(*N*-morpholino)ethanesulfonic acid; MOPS, 3-(*N*-morpholino)-propanesulfonic acid; SDS–PAGE: sodium dodecyl sulfate polyacrylamide gel electrophoresis.

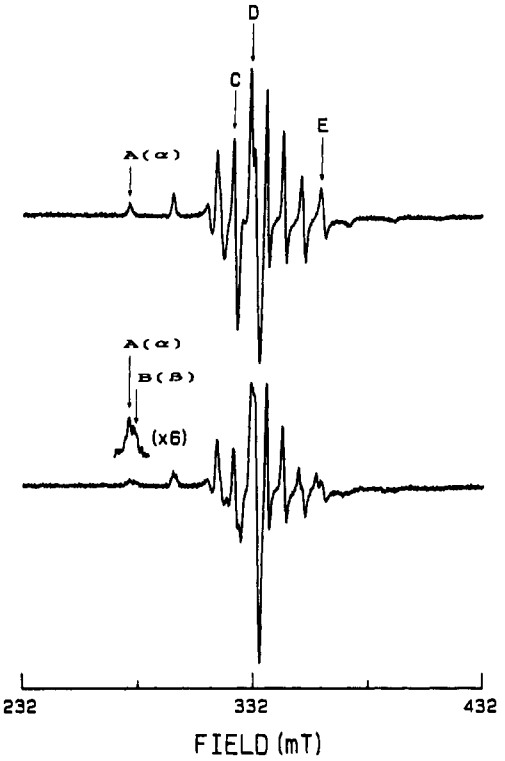

FIGURE 1: (Top) EPR spectrum of apoferritin containing 8 VO^{2+}/protein at pH 5.71 (0.93 mM VO^{2+}, 0.117 mM apoferritin, 0.15 M MES, 0.1 M NaCl). The labeled arrows A–E indicate fields for the α VO^{2+} complex at which ENDOR spectra were collected. (Bottom) EPR spectrum of apoferritin containing 16 VO^{2+}/protein at pH 7.36 (2.7 mM VO^{2+}, 0.169 mM apoferritin, 0.15 M HEPES, 0.1 M NaCl). The arrows labeled A and B indicate the α and β VO^{2+} species at the $M_I = -7/2$ parallel hyperfine component of the spectrum, respectively. Field positions marked A in the top and bottom spectra are the same. Spectrometer settings: microwave frequency, 9.37 GHz; microwave power, 5 mW; modulation frequency, 100 kHz; modulation amplitude, 2 G; temperature, 77 K.

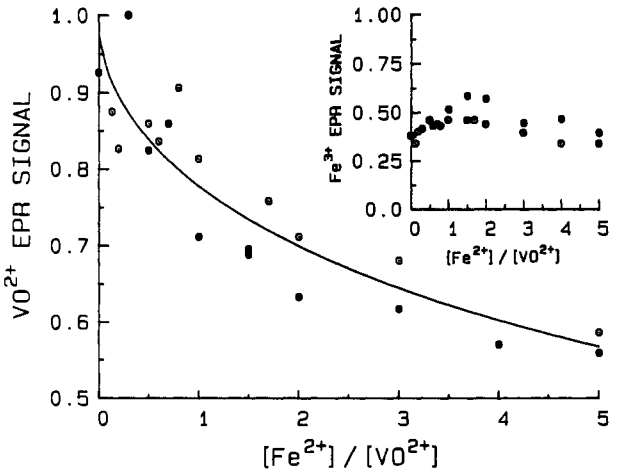

FIGURE 2: EPR spectrometric titration of apoferritin with Fe^{2+} and VO^{2+} in 0.15 M MOPS and 0.1 M NaCl, pH 7.0. The VO^{2+} signal intensity of the vandyl–protein complex (12 VO^{2+}/protein) was monitored as a function of the VO^{2+}/Fe^{2+} ratio. (Open symbols) Fe^{2+} added to VO^{2+}–apoferritin. (Closed symbols) VO^{2+} added to Fe^{2+}–apoferritin. (Inset) The residual $g' = 4.3$ Fe^{3+} signal amplitude [typically less than 0.3 Fe^{3+}/protein (Hanna et al., 1991)] was monitored simultaneously to ensure that no significant oxidation of the added Fe^{2+} had occurred. Spectrometer settings were the same as in Figure 1.

It can be readily shown that the concentration of vanadyl protein complex [VOP] is given by the positive root of the quadratic equation

$$[VOP] = [-b + (b^2 - 4ac)^{1/2}]/2a \quad (2)$$

where

$$a = K - 1 \quad (3)$$

$$b = K[VO]_0R - K[P]_0 + [P]_0 + [VO]_0 \quad (4)$$

$$c = -[P]_0[VO]_0 \quad (5)$$

and

$$R = [Fe]_0/[VO]_0 \quad (6)$$

Here $[P]_0$, $[VO]_0$, and $[Fe]_0$ are the analytical (total) concentrations of protein-binding sites, vanadium, and iron in the solution, respectively.

The EPR amplitude I as a function of the total iron(II) to vanadyl(IV) ratio R was least-squares fitted to eq 7 with [VOP] given by eq 2. The proportionality constant k and the equilibrium constant K were the only adjustable parameters (Figure 2, solid line).

$$I = k[VOP] \quad (7)$$

The data were successfully modeled with $k = 2.24 \pm 0.13$ and $K = 0.066 \pm 0.015$ (Figure 2, solid line). The results indicate that VO^{2+} binds 15 times more strongly to the protein than does Fe^{2+} ($1/K = 15$).

ENDOR Spectroscopy. In the ^{14}N ENDOR experiment, the electron–nuclear hyperfine interaction A_i ($i = x, y, z$ in the g-tensor coordinate system) is large compared to the ^{14}N nuclear Zeeman splitting. Thus, ^{14}N ENDOR resonances are centered at $|A_i|/2$ and split (to first order) by twice the nuclear free precessional frequency, ν_N. In addition, there is a quadrupole interaction, Q, since ^{14}N has a nuclear spin of 1, such that

$$\nu_{ENDOR} = (|A_i|/2) \pm \nu_N \bullet 3Q_i/2 \quad (8)$$

Thus, a single ^{14}N nucleus can give rise to four resonance peaks in the ENDOR spectrum. When resonances from more than one ^{14}N are present, the resulting ENDOR spectra may become quite complex and often only the major features can be identified.

ENDOR spectra of VO^{2+} collected below 10 MHz are shown in Figure 3 with $\mathbf{H}_0$ parallel ($m_I = -7/2$ $\parallel$ line, position A in Figure 1) and perpendicular ($m_I = +7/2$ $\perp$ line, position E) to the molecular z-axis. Here the z-axis is taken as the V=O bond direction. The multiple peaks at low frequency ($\nu_{ENDOR} \leq 7$ MHz) are consistent with the presence of ^{14}N couplings in the VO^{2+}–apoferritin complex. It is unlikely that any of these low frequency features are due to protons with $A > 12$ MHz since no ^1H lines were observed above 18 MHz where the high-frequency components of such strongly coupled protons would be expected to occur (see below). None of the spectral features were observed when ENDOR spectra were measured on buffer alone, indicating that the peaks in Figure 3 are from the protein and not the ENDOR cavity.

For comparison with VO^{2+}–apoferritin, ENDOR spectra were also taken of $VO^{2+}{}_2$–transferrin, which is known to have a single histidine ligand, the other ligands being oxygen donors (Eaton et al., 1989; Anderson et al., 1989). ENDOR spectra taken at the field positions of the parallel ($m_I = -7/2$ $\parallel$) and perpendicular ($m_I = +7/2$ $\perp$) EPR lines are shown in Figure 4. As with ferritin in Figure 3, transferrin exhibits complex patterns of ^{14}N resonances in the 1–7 MHz range. There are clearly many more lines than the four predicted by eq 8. In contrast to the case with the proteins, four lines are normally seen for simple VO^{2+} complexes such as vanadyl tetraphenylporphyrin or the pyridine adduct of vanadyl(acetylacetonate)$_2$ in which only a single type of nitrogen is present (Atherton et al., 1987; Kirste & van Willigen, 1982). We conclude that in the case of the proteins more than one ni-

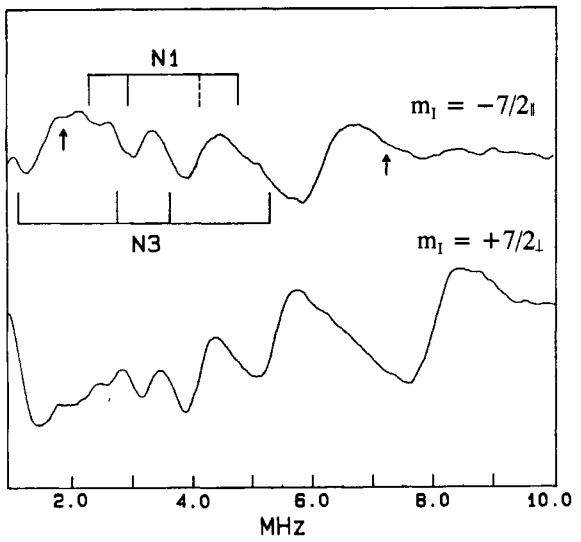

FIGURE 3: (Top) ^{14}N ENDOR spectra of the VO^{2+}–apoferritin complex at $g' = 2.41$ [position A in Figure 1 (top)]. (Bottom) ^{14}N ENDOR spectra of the VO^{2+}–apoferritin complex at $g' = 1.84$ [position E in Figure 1 (top)]. These positions correspond to the $M_I = -7/2$ line in the parallel region and the $M_I = +7/2$ line in the perpendicular region of the EPR spectrum, respectively. Stick diagrams show tentative assignments of ^{14}N lines. Arrows denote unassigned lines. Conditions were as in Figure 1 except the protein concentration was 42 μM. Spectrometer settings: microwave frequency, 9.449 GHz; microwave power, 20 mW; time constant, 200 ms; gain, 5×10^4; rf modulation frequency, 12.5 kHz; rf attenuation, 12 dB; rf modulation depth, 200 kHz; rf scan rate, 1 MHz/s; number of scans, 100; sample temperature, 2.3 K.

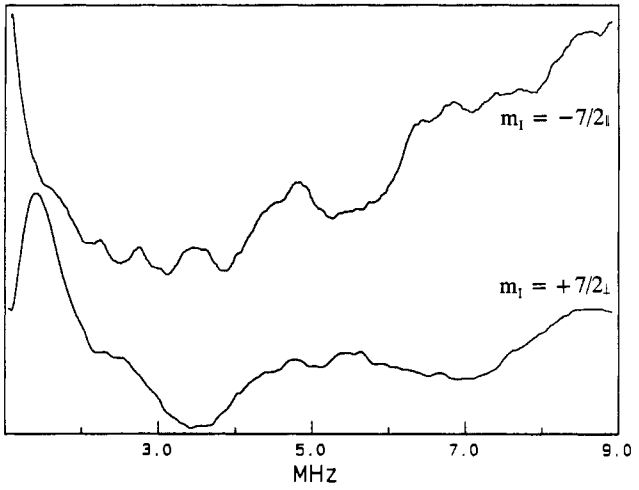

FIGURE 4: ^{14}N ENDOR of the $VO^{2+}{}_2$–transferrin complex. (Top) At the magnetic field position of the $m_I = -7/2 \parallel$ line ($g' = 2.39$). (Bottom) At the magnetic field position of the $m_I = +7/2 \perp$ line ($g' = 1.86$). The protein concentration was 1.5 mM in 0.1 M HEPES buffer, pH 7.4, under N_2. Spectrometer settings: microwave frequency, 9.4686 GHz; microwave power, 20 mW; time constant, 50 ms; gain, 5×10^4; rf modulation frequency, 12.5 kHz; rf attenuation, 12 dB; rf modulation depth, 100 kHz; rf scan rate, 2 MHz/s; number of scans, 2000 (top) and 100 (bottom); sample temperature, 2.0 K (top) and 2.3 K (bottom).

trogen, most likely two, contribute to the observed ^{14}N ENDOR pattern. Since there is only a single histidine in the binding site of transferrin, the observed lines appear to be from both the directly coordinated and remote nitrogens of the imidazole ring. The ENDOR spectra of the VO^{2+}–apoferritin complex can be interpreted similarly. Consistent with this interpretation is the observation that remote and coordinated nitrogens both contribute to the ENDOR spectra of vanadyl imidazole and carnosine complexes and have similar nuclear hyperfine coupling constants (Mulks et al., 1982). However,

Table I: ^{14}N ENDOR Results for H_0 Parallel to the V=O Bond

ligand	nitrogen[a]	A_z[b]	Q_z[b,c]	ref
apoferritin	N1	7.14	0.24	this work
	N3	6.36	0.85	
imidazole	N1*	7.40	0.23	Mulks et al., 1982
	N3	6.64	0.80	
histidine	N3*	6.00	0.76	Mulks et al., 1982
carnosine	N1*	7.10	0.24	Mulks et al., 1982
	N3	6.67	0.79	
pyridine	N*	6.50	0.85	Kirste & van Willigen, 1982
ammonia	N*	5.63	0.51	Kirste & van Willigen, 1982

[a] N1 and N3 refer to the sp^3 and sp^2 nitrogens of the imidazole ring, respectively, and the asterisk denotes the coordinating nitrogen. [b] In MHz. [c] See footnote 2.

the ENDOR spectra of VO^{2+}–apoferritin are not conclusive on this point, and the possibility that there are two different nitrogen ligands in this protein cannot be excluded.

The center of the ^{14}N line pattern for the parallel spectra [Figures 3 (top) and 4 (top)] of the proteins can be used to estimate values for the coupling constant A_z (eq 8). Values of $A_z \approx 7.4$ and 7.5 MHz are obtained for transferrin and ferritin, respectively. These values compare favorably with the coupling of 7.0 MHz observed by ESEEM for the imidazole ligand of VO^{2+}–transferrin (Eaton et al., 1989). In contrast, significantly smaller ^{14}N couplings of $\sim$5 MHz are expected for VO^{2+}–amine nitrogen coordination (Tipton et al., 1989). Thus, the gross features of the ^{14}N spectra of both transferrin and ferritin are in keeping with histidine as a ligand.

A detailed interpretation of the ^{14}N spectra of the proteins is complicated by a number of factors. The protein ENDOR lines are considerably broadened relative to those commonly found for small chelates. For example, the ^{14}N line widths of the vanadyl porphyrin complex are $\Delta\nu_{pp} \sim 0.2$ MHz (Atherton et al., 1987) compared with 0.6 MHz for ferritin. This observation suggests the presence of significant "A-strain" in the protein complexes and a distribution of ligand configurations about the metal in the frozen sample. Furthermore, the intensities of the ^{14}N lines vary considerably, making weak lines close to strong ones difficult to discern. Such marked variation in ENDOR intensity is observed in parallel field with simple chelates as well (Kirste & van Willigen, 1982; Atherton et al., 1987). For example, the weakest and strongest line of the quadruplet of vanadyl tetraphenylporphrin differ 6-fold in intensity (Atherton et al., 1987). Despite these complications, a possible assignment of the ENDOR spectrum of ferritin to two nitrogens for $H_0 \| z$ is indicated in Figure 3 (top). A similar assignment of lines to two nitrogen nuclei is not immediately evident in the transferrin spectrum, however (Figure 4, top). The more strongly coupled nitrogen in ferritin, labeled N1 in Figure 3 (top), has an A_z of 7.14 MHz and a quadrupole splitting Q_z of 0.24 MHz.[2] The more weakly coupled nitrogen, labeled N3, gave values of 6.36 and 0.85 MHz for A_z and Q_z, respectively. The strong resonance centered at 7.25 MHz and the low frequency resonance at 1.89 MHz, indicated by arrows, are unassigned.

The ^{14}N ENDOR parameters of VO^{2+}–apoferritin are summarized in Table I for $H_0 \| z$. For comparison, ^{14}N data obtained from other VO^{2+} complexes in which the nitrogen

[2] A_z is the electron–nuclear hyperfine coupling, and Q_z is the quadrupole coupling where z is taken as the V=O bond direction ($H_0 \| z$) and does not necessarily correspond to the principal z-axis of the quadrupole coupling tensor. It should be noted that the z-axis of the quadrupole tensor usually lies in the direction of the V–N bond for coordinated imidazoles (Ashby et al., 1978).

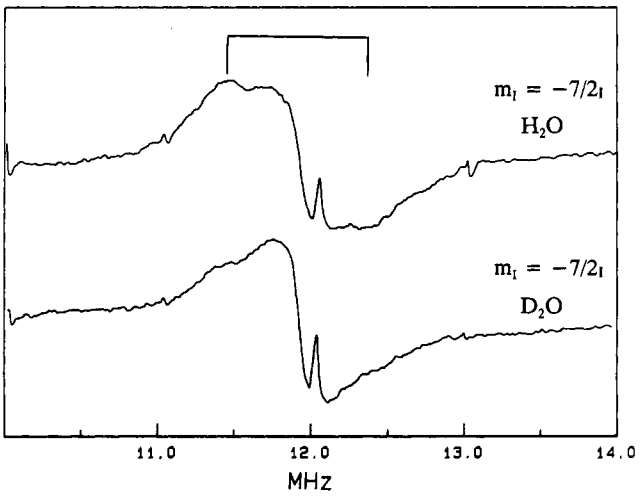

FIGURE 5: Proton ENDOR of the VO^{2+}–apoferritin complex at the magnetic field position A in Figure 1 ($g' = 2.41$) in H_2O (top) and D_2O (bottom). A coupling of 1 MHz is indicated. The solution conditions were as in Figure 1 (top) with pH 7.4 and pD 7.7. Spectrometer settings: microwave frequency, 9.4315 GHz; microwave power, 20 mW; time constant, 20 ms; gain, 5×10^4; rf modulation frequency, 12.5 kHz; rf attenuation, 12 dB; rf modulation depth, 75 kHz; rf scan rate, 1 MHz/s; number of scans, 2400 (top) and 1600 (bottom); sample temperature, 2.3 K.

is coordinated equatorially to the VO axis are also presented. The hyperfine and quadrupole couplings for VO^{2+}–apoferritin closely match those of the protonated N1 (sp^3) nitrogen and the N3 (sp^2) nitrogen of an imidazole ring coordinated to the vanadium in the equatorial plane.

The ^{14}N ENDOR spectra of the proteins shown in Figure 3 (bottom) and Figure 4 (bottom), when $\mathbf{H}_0$ is in the *xy*-plane, are much more difficult to intrepret since ligand hyperfine couplings from A_x and A_y for two nitrogens can contribute up to 16 lines to the spectrum not counting possible off-axis turning points.[2] The spectrum is also complicated by the line width and intensity factors mentioned above and by partial powder pattern effects since a single orientation of the VO^{2+} complex relative to $\mathbf{H}_0$ are not obtained at perpendicular field settings. Interpretation of ^{14}N ENDOR in perpendicular field orientation can be problematic even in simple complexes (Kirste & van Willigen, 1982). Because of the complexity of the perpendicular spectrum, a detailed assignment was not attempted.

Further evidence for the assignment of the ENDOR spectrum of VO^{2+}–apoferritin to histidine comes from proton ENDOR. In the ^1H ENDOR experiment, the nuclear Zeeman energy is large compared to the electron–nuclear hyperfine energy. Thus, ENDOR resonances appear (to first order) at

$$\nu_{ENDOR} = \nu_P \pm |A_i|/2 \qquad (9)$$

where A_i is the proton nuclear hyperfine coupling constant and ν_P is the proton free precessional frequency at the given magnetic field. Two ENDOR lines having a splitting of A_i are predicted by eq 9. Figure 5 shows proton ENDOR spectra taken at field position A, $\mathbf{H}_0 \| z$, for samples in H_2O and D_2O. Upon D_2O–H_2O exchange, collapse of ENDOR intensity from an exchangeable proton(s) with a coupling of approximately 1 MHz is apparent. A 1 MHz coupling due to the coordinated NH group is observed in the ENDOR spectrum of a VO^{2+} imidazole complex in parallel field orientation and is similarly lost upon D_2O–H_2O exchange (Mulks et al., 1982). For perpendicular field orientation, no loss of proton couplings in the ferritin spectrum was observed upon D_2O–H_2O exchange (data not shown). This result is also in accord with the finding for VO^{2+} imidazole where the proton coupling of the NH group was not resolved from the proton matrix line in perpendicular field (Mulks et al., 1982). In addition, there is a coupling of 2.02 MHz from a weak pair of lines at 11 and 13 MHz in Figure 5 that we assign to nonexchangeable proton(s) of protein ligands. VO^{2+}–imidazole shows a coupling of 2.7 MHz from the H2 proton of the imidazole ring (Mulks et al., 1982).

The overall intensity of the large ^1H matrix line in perpendicular field orientation of the VO^{2+}–apoferritin complex, estimated as $\Delta H_{pp}{}^2 Y$ (where ΔH_{pp} and Y are the peak-to-peak width and height, respectively), decreased by about 35% for samples prepared in D_2O. Thus the metal site is clearly accessible to solvent. Exchangeable protons on the protein as well as outer-sphere water in the vicinity of the vanadyl ion presumably account for the loss in intensity of the matrix peak in D_2O. However, no ^2H resonances were observed for samples in D_2O. Weak ENDOR signals typical of strongly coupled protons ($A > 5$ MHz) of first coordination sphere aquo ligands were not observed with any of the samples. They would be difficult to see at the concentrations employed in the present work (Mustafi & Makinen, 1988; van Willigen, 1980).

Discussion

The binding of both Fe^{3+} and Fe^{2+} to apoferritin is now well established (Rosenberg & Chasteen, 1982; Chasteen et al., 1985; Hanna et al., 1991; Chasteen & Theil, 1982; Yang et al., 1989; Jacobs et al., 1989; Watt et al., 1985; Wardeska et al., 1986) as is the interaction between apoferritin and VO^{2+} (Wardeska et al., 1986; Chasteen & Theil, 1982; Chasteen et al., 1986a,b). The addition of VO^{2+} to apoferritin containing either Fe^{2+} (Figure 2) or Fe^{3+} (Chasteen & Theil, 1982) shows competitive binding between the metals and suggests a common binding site or binding region on the protein for all three. The same site is also common to α and β forms of VO^{2+}–apoferritin since ENDOR data (not shown) did not reveal any major spectroscopic differences between the forms, and EPR spectrometric titrations showed that the relative amounts of α and β EPR signals remain constant as VO^{2+} is added to the protein.

The ENDOR experiment provides insight into the metal site in VO^{2+}–apoferritin. Although we are not yet able to interpret the ENDOR spectra fully, the important conclusion of the present work is that the metal site involves nitrogen coordination, probably from the imidazole ring of a histidine residue. This finding contrasts with the generally held idea that the iron-binding sites in horse spleen ferritin involve carboxylate groups or other oxygen donor ligands. The results of the present study indicate that VO^{2+} cannot bind *within* the protein 3-fold hydrophilic channels as previously proposed from binding stoichiometries (Wardeska et al., 1986) since these channels do not contain residues with N-donor ligands (Ford et al., 1984). The significant decrease (30–40%) in the matrix line from D_2O–H_2O exchange indicates that the vanadyl ion is accessible to solvent and, therefore, to molecular oxygen. It is unlikely that the two nitrogens observed in the ENDOR (Figure 3) arise from VO^{2+} binding at two different sites since, within the resolution of the EPR spectrum, only a single species appears to be present (Figure 1, top).

A VO^{2+}-binding site with coordinating ligands from one histidine and two or three carboxylate residues seems most probable from the ENDOR results reported here and from EPR and ESEEM data (Chasteen & Theil, 1982; Gerfin et al., 1991). While a ferroxidase site having this ligand composition (Lawson et al., 1989; Levi et al., 1988, 1989) has been identified in human ferritin H-chain subunits [M_r 21 000

(Arosio et al., 1978)], the low percentage of H-subunits (4%) in horse spleen ferritin and the stoichiometry of VO^{2+} binding [up to ~16 VO^{2+}/protein (Wardeska et al., 1986)] preclude assignment of a VO^{2+} spectrum to an H-subunit site. Thus, it seems likely that the VO^{2+}- and Fe^{2+}/Fe^{3+}-binding site identified here is located on the L-chain subunits [M_r 19 000 (Arosio et al., 1978)], which in general comprises 90% or more of the horse spleen apoprotein structure.

X-ray crystal studies of horse spleen apoferritin have revealed a potential metal-binding site at His-132 and Asp-135′ (the prime indicating an adjacent subunit) on the interior surface of the protein near, but not within, the 3-fold hydrophilic channels (Harrison et al., 1986). This site binds Cd^{2+}, Zn^{2+}, and possibly Tb^{3+} (Harrison et al., 1986), which have been shown to compete with both Fe^{2+} and Fe^{3+} for protein-binding sites (Wardeska et al., 1986; Stefanini et al., 1989) and to inhibit iron uptake as well (Treffry & Harrison, 1984; Clegg et al., 1980a,b). Sites closely related by 3-fold symmetry could account for the metal-binding stoichiometries of 1 VO^{2+} and 2 VO^{2+} per 3 subunits reported earlier (Wardeska et al., 1986).

A mixed N–O donor set of ligands would be expected for a site that binds both Fe^{2+} and Fe^{3+}. It seems likely that the Fe^{2+}/Fe^{3+} site identified here facilitates the oxidation of Fe^{2+} during the initial stages of iron deposition in apoferritin. It has been suggested that human L-chain subunits, however, do not promote Fe^{2+} oxidation relative to normal autoxidation on the basis of a color development assay (Levi et al., 1989). A comparison of the amino acid sequences for horse spleen and human L-chain subunits show that both contain the residues His-132 and Asp-135 (horse spleen sequence numbering), but Ser-131 in the horse spleen sequence has been replaced by a threonine residue in the human L-chain sequence (Theil, 1989, and references therein), possibly accounting for differences in behavior of the two proteins.

Added in Proof

^{14}N ENDOR has been recently reported for VO^{2+}-substituted D-xylose isomerase. The ^{14}N coupling constant $A_z = 13.2$ MHz obtained from a tentative assignment of the spectrum is significantly larger than the value reported here for VO^{2+}–apoferritin ($A_z \sim 7$ MHz) and more closely corresponds to a value expected for axial ligation of the histidine nitrogen (Bogumil et al., 1991).

Acknowledgments

We thank Ms. Shujun Sun for performing the SDS–PAGE and Mr. John Grady for assistance in preparing the figures.

Registry No. Fe, 7439-89-6; VO, 20644-97-7; N, 7727-37-9.

References

Adelman, T. G., Arosio, P., & Drysdale, J. (1975) *Biochem. Biophys. Res. Commun. 63*, 1056–1062.

Anderson, B. F., Baker, H. M., Norris, G. E., Rice, D. W., & Baker, E. N. (1989) *J. Mol. Biol. 209*, 711–734.

Arosio, P., Adelman, T. J., & Drysdale, J. W. (1978) *J. Biol. Chem. 253*, 4451–4458.

Ashby, C. I. H., Cheng, C. P., & Brown, T. L. (1978) *J. Am. Chem. Soc. 100*, 6057–6063.

Atherton, N. M., Fairhurst, S. A., & Hewson, G. J. (1987) *Magn. Reson. Chem. 25*, 829–830.

Bogumil, R., Hüttermann, J., Kappl, R., Stabler, R., Sudfeldt, C., & Witzel, H. (1991) *Eur. J. Biochem. 196*, 305–312.

Bryce, C. F. A., & Crichton, R. R. (1973) *Biochem. J. 133*, 301–309.

Cannon, J. C., & Chasteen, N. D. (1975) *Biochemistry 14*, 4573–4577.

Chasteen, N. D. (1981) in *Biological Magnetic Resonance* (Berliner, L. J., & Reuben, J., Eds.) Vol. 3, pp 53–119, Plenum Press, New York.

Chasteen, N. D. (1983) *Struct. Bonding (Berlin) 53*, 105–138.

Chasteen, N. D., & Theil, E. C. (1982) *J. Biol. Chem. 257*, 7672–7677.

Chasteen, N. D., Antanaitis, B. C., & Aisen, P. (1985) *J. Biol. Chem. 260*, 2926–2929.

Chasteen, N. D., Lord, E. M., & Thompson, H. J. (1986a) in *Frontiers in Bioinorganic Chemistry* (Xavier, A., Ed.) pp 133–141, VCH Publishers, Weinheim, FRG.

Chasteen, N. D., Lord, E. M., Thompson, H. J., & Grady, J. K. (1986b) *Biochim. Biophys. Acta 884*, 84–92.

Clegg, G. A., Fitton, J. E., Harrison, P. M., & Treffry, A. (1980a) *Prog. Biophys. Mol. Biol. 36*, 53–86.

Clegg, G. A., Stansfield, D. K., Bourne, P. E., & Harrison, P. M. (1980b) *Nature 288*, 298–300.

Crichton, R. R. (1973) *Struct. Bonding (Berlin) 17*, 66–134.

Crichton, R. R., & Roman, F. (1978) *J. Mol. Catal. 4*, 75–82.

Eaton, S. S., Dubach, J., More, K. M., Eaton, G. R., Thurman, G., & Ambruso, D. R. (1989) *J. Biol. Chem. 264*, 4776–4781.

Ford, G. C., Harrison, P. M., Rice, D. W., Smith, J. M. A., Treffry, A., White, J. L., & Yariv, J. (1984) *Philos. Trans. R. Soc. London, B 304*, 551–565.

Gerfin, G. J., Hanna, P. M., Chasteen, N. D., & Singel, D. J. (1991) *J. Am. Chem. Soc. 113* (in press).

Hanna, P. M., Chen, Y., & Chasteen, N. D. (1991) *J. Biol. Chem. 266*, 886–893.

Harrison, P. M., Ford, G. C., Rice, D. W., Smith, J. M. A., Treffry, A., & White, J. L. (1986) in *Frontiers in Bioinorganic Chemistry* (Xavier, A., Ed.) pp 268–277, VCH Publishers, Weinheim, FRG.

Heusterspreute, M., & Crichton, R. R. (1981) *FEBS Lett. 129*, 322–327.

Jacobs, D., Watt, G. D., Frankel, R. B., & Papaefthymiou, G. C. (1989) *Biochemistry 28*, 9216–9221.

Kirste, B., & van Willigen, H. (1982) *J. Phys. Chem. 86*, 2743–2749.

Lawson, D. M., Treffry, A., Artymiuk, P. J., Harrison, P., Yewdall, S. J., Luzzago, A., Cesareni, G., Levi, S., & Arosio, P. (1989) *FEBS Lett. 254*, 207–210.

Lawson, D. M., Artymiuk, P. J., Yewdall, S. J., Smith, J. M. A., Livingstone, J. C., Treffry, A., Luzzago, A., Levi, S., Arosio, P., Cesareni, G., Thomas, C. D., Shaw, W. V., & Harrison P. (1991) *Nature 349*, 541–544.

Levi, S., Luzzago, A., Cesareni, G., Cozzi, A., Franceschinelli, F., Albertini, A., & Arosio, P. (1988) *J. Biol. Chem. 263*, 18086–18092.

Levi, S., Salfeld, J., Franceschinelli, F., Cozzi, A., Dorner, M. H., & Arosio, P. (1989) *Biochemistry 28*, 5179–5184.

Macara, I. G., Hoy, T. G., & Harrison, P. M. (1972) *Biochem. J. 126*, 151–162.

Mulks, C. F., Kirste, B., & van Willigen, H. (1982) *J. Am. Chem. Soc. 104*, 5906–5911.

Mustafi, D., & Makinen, M. W. (1988) *Inorg. Chem. 27*, 3360–3368.

Paques, E. P., Paques, A., & Crichton, R. R. (1979) *J. Mol. Catal. 5*, 363–375.

Rosenberg, L. P., & Chasteen, N. D. (1982) in *The Biochemistry and Physiology of Iron* (Saltman, P., & Hegenauer, J., Eds.) pp 405–407, Elsevier/North-Holland Biomedical Press, Amsterdam.

Stefanini, S., Desideri, A., Vecchini, P., Drakenberg, T., & Chiancone, E. (1989) *Biochemistry 28*, 378–382.
Theil, E. C. (1987) *Annu. Rev. Biochem. 56*, 289–315.
Theil, E. C. (1989) *Adv. Enzymol. Relat. Areas Mol. Biol. 63*, 421–449.
Tipton, P. A., McCracken, J., Cornelius, J. B., & Peisach, J. (1989) *Biochemistry 28*, 5720–5728.
Treffry, A., & Harrison, P. M. (1984) *J. Inorg. Biochem. 21*, 9–20.
Treffry, A., Harrison, A., Luzzago, A., & Cesareni, G. (1989) *FEBS Lett. 247*, 268–272.
van Willigen, H. (1980) *J. Magn. Reson. 39*, 37–46.
Wardeska, J. G., Viglione, B., & Chasteen, N. D. (1986) *J. Biol. Chem. 261*, 6677–6683.
Watt, G. D., Frankel, R. B., & Papaefthymoiu, G. C. (1985) *Proc. Natl. Acad. Sci. U.S.A. 82*, 3640–3643.
Yang, C. Y., Meagher, A., Huynh, B. H., Sayers, D. E., & Theil, E. C. (1989) *Biochemistry 26*, 497–503.

Secondary Structure and Side-Chain ^1H and ^{13}C Resonance Assignments of Calmodulin in Solution by Heteronuclear Multidimensional NMR Spectroscopy†

Mitsuhiko Ikura,‡ Silvia Spera,‡,§ Gaetano Barbato,‡,∥ Lewis E. Kay,‡ Marie Krinks,⊥ and Ad Bax*,‡

Laboratory of Chemical Physics, National Institute of Diabetes and Digestive and Kidney Diseases, and Laboratory of Biochemistry, National Cancer Institute, National Institutes of Health, Bethesda, Maryland 20892

Received April 9, 1991; Revised Manuscript Received June 28, 1991

ABSTRACT: Heteronuclear 2D and 3D NMR experiments were carried out on recombinant *Drosophila* calmodulin (CaM), a protein of 148 residues and with molecular mass of 16.7 kDa, that is uniformly labeled with ^{15}N and ^{13}C to a level of >95%. Nearly complete ^1H and ^{13}C side-chain assignments for all amino acid residues are obtained by using the 3D HCCH-COSY and HCCH-TOCSY experiments that rely on large heteronuclear one-bond scalar couplings to transfer magnetization and establish through-bond connectivities. The secondary structure of this protein in solution has been elucidated by a qualitative interpretation of nuclear Overhauser effects, hydrogen exchange data, and $^3J_{HNH\alpha}$ coupling constants. A clear correlation between the $^{13}C\alpha$ chemical shift and secondary structure is found. The secondary structure in the two globular domains of *Drosophila* CaM in solution is essentially identical with that of the X-ray crystal structure of mammalian CaM [Babu, Y., Bugg, C. E., & Cook, W. J. (1988) *J. Mol. Biol. 204*, 191–204], which consists of two pairs of a "helix–loop–helix" motif in each globular domain. The existence of a short antiparallel β-sheet between the two loops in each domain has been confirmed. The eight α-helix segments identified from the NMR data are located at Glu-6 to Phe-19, Thr-29 to Ser-38, Glu-45 to Glu-54, Phe-65 to Lys-77, Glu-82 to Asp-93, Ala-102 to Asn-111, Asp-118 to Glu-127, and Tyr-138 to Thr-146. Although the crystal structure has a long "central helix" from Phe-65 to Phe-92 that connects the two globular domains, NMR data indicate that residues Asp-78 to Ser-81 of this central helix adopt a nonhelical conformation with considerable flexibility.

Recent progress in NMR methodology has made it possible to obtain complete ^1H, ^{13}C, and ^{15}N resonance assignments for proteins in the 15–25-kDa molecular mass range, which constitutes a prerequisite for determining the 3D solution structure. Isotope-editing techniques combined with 2D NMR have been used successfully for recombinant proteins such as staphylococcal nuclease (18 kDa) (Torchia et al., 1989; Wang et al., 1990), *Escherichia coli* Trp repressor (a symmetric dimer of 25 kDa with 107 residues) (Arrowsmith et al., 1990), and T4 lysozyme (18.7 kDa) (McIntosh et al., 1990). This type of approach requires preparation of a large number of protein samples with selective isotope labeling of different amino acid types in the various protein preparations, a labor intensive and time-consuming process. More recent approaches, on the other hand, utilize uniform labeling with ^{15}N or ^{13}C in combination with 2D and 3D techniques. The 3D NOESY-HMQC experiment is an important example of this

Table I: Location of α-Helices in Calmodulin-$4Ca^{2+}$ Determined by NMR and X-ray Diffraction

α-helix	residue range	
	NMR[a]	X-ray[b]
I	E6–F19	T5–F19
II	T29–S38	T29–S38
III	E45–E54	E45–V55
IV	F65–K77	F65–F92
V	E82–D93	
VI	A102–N111	A102–N111
VII	D118–E127	D118–A128
VIII	Y138–T146	Y138–S147

[a] Present work. The experimental conditions are 0.1 M KCl, pH 6.3, at 36 °C. [b] Babu et al. (1988). The crystals were obtained from 45–60% (v/v) 2-methyl-2,4-pentanediol containing 50 mM cacodylate buffer, pH 5.6.

† This work was supported by the Intramural AIDS-Directed Antiviral Program of the Office of the Director of the National Institutes of Health. L.E.K. acknowledges a Centennial Fellowship from the Medical Research Council of Canada and the Alberta Heritage Trust Foundation. G.B. acknowledges a fellowship from Facolta di Scienze, Napoli Dottorato di Ricerca in Scienze Chimiche.

* To whom correspondence should be addressed.
‡ NIDDK, NIH.
§ Present address: Istituto Guido Donegani, Via Fauser 4, Novara, Italy.
∥ On leave from Universita di Napoli, Federico II, Dipartimento di Chimica, Via Mezzocannone 4, Naples, Italy.
⊥ National Cancer Institute, NIH.

0006-2960/91/0430-9216$02.50/0